PHYSICAL REVIEW A VOLUME 53, NUMBER 6 JUNE 1996

Vibrational branching ratios for single-photon ionization of Na_2

Henrik Rudolph
Debye Institute, Utrecht University, P.O. Box 80000, 3508 TA Utrecht, The Netherlands

Xavier Urbain
Departement de Physique, Université Catholique de Louvain, Chemin du Cyclotron 2, 1348 Louvain-la-Neuve, Belgium

(Received 18 September 1995; revised manuscript received 25 January 1996)

We report on an *ab initio* study of the single-photon ionization of Na_2 from the electronic ground state ($X\ ^1\Sigma_g^+$) and subsequent photodissociation of the resulting ion. The calculations are done as a function of internuclear distance ($R=4.5$–7.5 a.u.) and for a range of photoelectron energies 0.25–10 eV. The electronic continuum wave functions are determined using the so-called iterative Schwinger method, which is an L^2 method based on a single-center expansion of all relevant operators and wave functions. A Cooper minimum is found in the $k\pi$-continuum's p wave ($l=1$) around a photoelectron energy of approximately 4.5 eV. This does not, however, lead to significant observable implications for the total cross sections. The subsequent photodissociation of the $Na_2{}^+$ ions is calculated using a numerical Numerov method, based on previously calculated data for the molecular potential-energy curves and dipole matrix elements. The spectrum resulting from photodissociation of ions created via photoionization of a thermal distribution of Na_2 molecules is calculated and compared with the recent results of Kortyna *et al.* [Phys. Rev. A **50**, 1399 (1994)]. Excellent agreement is found with the experimental values if the assumed initial temperature of the molecular beam is approximately 50 K, which is substantially colder than previously estimated. [S1050-2947(96)08005-5]

PACS number(s): 33.80.Eh, 31.15.Ar, 33.80.Gj, 33.60.−q

I. INTRODUCTION

The sodium-sodium collisional system and the Na_2 molecule have in recent years received much attention, since the sodium atom is a prototypical pseudo-single-electron system and furthermore easily manipulated with current dye laser technologies [1–5]. In two recent papers the ionic vibrational distributions have been experimentally determined for the associative ionization (AI) process [$\mathrm{Na}(3p)+\mathrm{Na}(3p)\rightarrow \mathrm{Na}_2{}^+(v^+,J^+)+e^-$] [6] and the single-photoionization (PI) process [$\mathrm{Na}_2(X\ ^1\Sigma_g^+)+h\nu\rightarrow \mathrm{Na}_2{}^+(v^+,J^+)+e^-$] [7]. It was found that there was a substantial population inversion for the AI process, whereas a large vibrational excitation was not found in the PI experiments, since these were done with a photon energy equivalent to the adiabatic ionization potential (V_{IP}) of Na_2 [7].

In the present paper we study the single-photoionization process using an *ab initio* method based on a combination of a Hartree-Fock method for the determination of the bound states of Na_2 and for the calculation of the electronic continuum wave functions the so-called iterative Schwinger method, which is implemented in a single-center expansion formalism [8,9]. The dynamical quantities, cross sections, and dipole matrix elements, are calculated as a function of internuclear distance (4.5–7.5 a.u.) and are vibrationally averaged to allow a more comprehensive comparison with experimental results. The rather shallow potential well of the ground state of Na_2 with classical turning points for, e.g., $v=3$ of approximately $R_{\mathrm{inner}}=5.208$ a.u. and $R_{\mathrm{outer}}=6.585$ a.u. and similarly for the ionic state, requires special attention since the vibrational wave functions are unusually extended [10].

II. THEORY AND COMPUTATIONAL DETAILS

The photoionization process of Na_2

$$\mathrm{Na}_2(X\ ^1\Sigma_g^+(v,J))\xrightarrow{h\nu}\mathrm{Na}_2{}^+(X\ ^2\Sigma_g^+(v^+,J^+))+e^- \qquad (1)$$

is conceptually thought of as a single-step process leading to an ion in the electronic ground state with a given vibrational and rotational excitation and a photoelectron [8]. The determination of the total process therefore requires the description of the initial bound molecular ground state and the final ionic state, combined with the continuum electron wave function [9].

The bound-state electronic wave function is calculated using the GAMESS computer program [11], using the uncontracted basis set tabulated in Table I. This basis leads to a total energy of −323.707 90 a.u. for an internuclear distance of 6.0 a.u. The equilibrium distance determined in this approximation is 6.039 a.u. with a harmonic vibrational constant $\omega_0=157.56\ \mathrm{cm}^{-1}$. The corresponding experimental values are 5.818 a.u. for the equilibrium distance and for the vibrational constant $\omega_0=159.17\ \mathrm{cm}^{-1}$ [12]. The electronic wave function is calculated for seven values of R from 4.5 to 7.5 a.u. with steps of 0.5 a.u., which is more than sufficient to cover all of the classically allowed region for the ten lowest vibrational states of the ground state [10]. The electronic wave function has also been determined with more sophisticated methods [multiconfiguration self-consistent field (MSCF)], but the shape of the potential well and the equilibrium distance determined were not found to be significantly different. The SCF level was therefore deemed to be sufficient for the present description, despite the large range of R values necessary.

TABLE I. Gaussian basis set used for the SCF calculation of the electronic ground state of Na_2 and $Na_2{}^+$.

Type	Exponent
s	36 166.4
s	5372.58
s	1213.21
s	339.62
s	109.55
s	38.777
s	14.576
s	5.2699
s	1.8278
s	0.6199
s	0.0572
s	0.0240
p	144.645
p	33.907
p	10.629
p	3.8239
p	1.4443
p	0.5526
p	0.1887
p	0.0465
p	0.0163
d	0.7000
d	0.1750
d	0.043 75

The electronic ground state of Na_2 has, in a one-electron description, the electronic configuration $1\sigma_g^2 1\sigma_u^2 2\sigma_g^2 2\sigma_u^2 1\pi_g^4 1\pi_u^4 3\sigma_g^2 3\sigma_u^2 4\sigma_g^2$ and the $Na_2{}^+$ ground state has the electronic configuration $1\sigma_g^2 1\sigma_u^2 2\sigma_g^2 2\sigma_u^2 1\pi_g^4 1\pi_u^4 3\sigma_g^2 3\sigma_u^2 4\sigma_g^1$. Since the ionization is from the $4\sigma_g$ orbital, the continuum electron is of either σ_u or π_u symmetry and only odd partial waves ($l=1,3,5,\ldots$) therefore contribute to the electronic continuum wave function in a single-center expansion around the center of mass of the Na_2 molecule. To determine the electronic continuum wave function we have used the so-called iterative Schwinger method, which has in the past been used very successfully for a variety of systems [8,9,13,14]. The current implementation of the iterative Schwinger variational method is a single-center expansion method where all pertinent quantities are determined in an l expansion and on a radial grid [8]. The radial grid used has 800 points ranging out to 67.9 a.u. with a varying grid distance, from 0.005 a.u. close to the origin to a grid distance of 0.16 a.u. close to the end points. This large grid far exceeds the extent of either of the bound states and ensures an adequate description of the wave functions. For the expansion of the bound molecular orbitals a maximum partial wave of 90 was used for the direct potential and the maximum partial wave for the exchange potential is 90 ($1\sigma_g$), 90 ($1\sigma_u$), 80 ($2\sigma_g$), 65 ($2\sigma_u$), 55 ($3\sigma_g$), 50 ($1\pi_u$), 50 ($1\pi_g$), 30 ($3\sigma_g$), and 20 ($4\sigma_g$), respectively. For the expansion of $1/r_{12}$ in the direct term, 180 partial waves were used and 90 in the exchange term. All other partial wave expansions were truncated at $l=90$. This ensures a normalization of the various bound orbitals for all distances to better than 98.8% and for all orbitals, except the $1\sigma_g$ and $1\sigma_u$ orbitals, better than 99.9%. In Table II the orbital expansions are listed for the various orbitals for (a) $R=4.5$ a.u. and (b) $R=7.5$ a.u., respectively. It is seen from Table II that there is not a significant orbital evolution for the $4\sigma_g$ state as a function of the internuclear distance and that it has a predominant s character of 91.81% and 92.90% at $R=4.5$ and 7.5 a.u., respectively. This strong Rydberg character has significant implications on the photoionization dynamics; see later.

The photoelectron continuum wave function is determined at the Hartree-Fock level in the frozen core approximation, where it is assumed that the ionic core after the photoionization is identical to the $N-1$ electron core of the ground state [8]. The photoelectron wave function φ_k is the solution to the one-electron Schrödinger equation

$$\left[-\frac{1}{2}\nabla^2+V_{N-1}(\mathbf{r},R)-\frac{k^2}{2}\right]\varphi_k(\mathbf{k},R)=0, \tag{2}$$

where $V_{N-1}(\mathbf{r},R)$ is the static-exchange potential of the molecular ion charge density, $k^2/2$ is the photoelectron kinetic energy, and φ_k satisfies the appropriate scattering boundary conditions. The photoelectron wave function of Eq. (2), φ_k, is determined using the iterative Schwinger method, which has been described elsewhere in greater detail [8,9,13,14], and we refer the reader to these references for further details and will here give only details pertaining to the present study. This method is implemented in a single-center formalism where all relevant operators and wave functions are expanded in a partial-wave expansion. In this formalism φ_k is therefore given by

$$\varphi_k(\mathbf{r})=\left(\frac{2}{\pi}\right)^{1/2}\sum_{l=0}\sum_{m=-l}^{l} i^l\Psi_{klm}(r)Y_{lm}^*(\hat{k}). \tag{3}$$

Equation (2) is iteratively solved by first guessing a solution based on a wave function created by augmenting the pure Coulomb waves for a given value of k with a number of discrete basis functions, which are effective in representing the molecular nature of the continuum wave function close to the nuclei. To ensure a fast convergence we have used an unusually large scattering basis set, which is listed in Table III [14]. We have allowed for three iterations, but the calculations were for all internuclear distances converged to better than within 4% of the final result after two iterations. A maximum value of 11 was used for the l expansion of the continuum electron wave function, which proved to be more than sufficient due to the strong Rydberg character of the $4\sigma_g$ state of the Na_2 ground state.

For the vibrational averaging of the dipole transition moment and the photodissociation dynamics the one-dimensional Schrödinger equation was solved using a Numerov method [15], with a grid of 1001 points, an inner turning point of 4.55 a.u., and an outer turning point of 8.10 a.u. for the ground state of the neutral molecule and a grid with 2001 points, an inner turning point of 4.55 a.u., and an outer turning point of 11.65 a.u. for the ground state of the ion. For the electronic potentials of the bound states we used

TABLE II. Single-center expansion coefficient (in percentage) for the various occupied molecular orbitals of Na_2 for an internuclear distance of (a) 4.5 a.u. and (b) 7.5 a.u. Due to the inversion symmetry of the Na_2 molecule the gerade and ungerade orbitals are listed separately.

(a) 4.5 a.u.

Gerade	$l=0$	$l=2$	$l=4$	$l=6$	$l=8$	Sum
$1\sigma_g$	0.92	4.43	7.25	9.1	9.94	31.64
$2\sigma_g$	20.83	46.16	19.89	4.67	0.97	92.52
$3\sigma_g$	19.4	34.28	22.83	12.14	5.83	94.48
$1\pi_g$		22.44	31.11	21.19	11.77	86.51
$4\sigma_g$	91.81	6.01	1.65	0.23	0.03	99.73
Ungerade	$l=1$	$l=3$	$l=5$	$l=7$	$l=9$	Sum
$1\sigma_u$	2.73	5.95	8.3	9.64	10.03	36.65
$2\sigma_u$	46.18	33.71	10.22	2.03	0.7	92.84
$1\pi_u$		8.42	30.64	26.67	15.92	81.65
$3\sigma_u$	36.39	29.64	17.34	8.63	4.11	96.11

(b) 7.5 a.u.

Gerade	$l=0$	$l=2$	$l=3$	$l=6$	$l=8$	Sum
$1\sigma_g$	0.33	1.64	2.85	3.90	4.75	13.47
$2\sigma_g$	7.48	27.91	27.25	17.08	8.07	87.79
$3\sigma_g$	6.38	21.92	22.27	17.07	11.67	79.31
$1\pi_g$		25.49	15.52	19.34	17.14	77.49
$4\sigma_g$	92.90	3.52	1.97	0.97	0.34	99.70
Ungerade	$l=1$	$l=3$	$l=5$	$l=7$	$l=9$	Sum
$1\sigma_u$	0.99	2.26	3.40	4.35	5.09	16.09
$2\sigma_u$	20.03	29.70	22.52	12.08	5.14	89.47
$1\pi_u$		1.44	10.85	18.40	18.72	49.41
$3\sigma_u$	16.56	23.34	19.91	14.26	9.43	83.50

the previously published, experimentally determined, RKR potentials for the ground state [10] and the ion ground state [7].

III. RESULTS

In Fig. 1 the absolute value of the dipole transition matrix element $|r_{fi}^{l\lambda\mu}|$ is shown as a function of the kinetic energy for various partial waves for an internuclear distance of 6.0 a.u., where $r_{fi}^{l\lambda\mu}$ is given by

$$r_{fi}^{l\lambda\mu}=\sum_{l',l}\langle\Psi_{ll'\lambda}(r)Y_{l'\lambda}(\hat{r})|rY_{1\mu}(\hat{r})|\varphi_{il_0}(r)Y_{l_0\lambda-\mu}(\hat{r})\rangle, \tag{4}$$

where Ψ is the bound state, r the dipole moment operator, and φ the continuum wave function, all expressed in the single-center expansion formalism. The photoionization transition moment is, in the dipole-length form, given by [8]

$$I_{lm\mu}(R,k)=k^{1/2}\langle\Psi_i(r,R)|r_\mu|\Psi_{klm}(r,R)\rangle \tag{5}$$

and the vibrationally averaged cross section (in the dipole-length form) is therefore given by [8]

$$\sigma_{v,v'}=\frac{4\pi^2E}{3c}\sum_{l,m,\mu}|\langle\chi_i^v|I_{lm\mu}(R,k_{v,v^+})|\chi_f^{v^+}\rangle|^2, \tag{6}$$

where $k_{v,v^+}=[2(E-V_{\mathrm{IP}}+E_v-E_{v^+})]^{1/2}$ and χ_i,χ_f are the vibrational wave functions for the ground states of the neutral atom and the ion, respectively. E is the photon energy and c is the speed of light. The photoionization transition moments $I_{lm\mu}(R,k)$ have been evaluated for each internuclear distance for a range of kinetic energies of the final photoelectron up to a maximum kinetic energy of 10 eV, as indicated in Fig. 1. For the evaluation of the vibrationally

TABLE III. Scattering basis set used in the iterative Schwinger method for the determination of the photoelectron continuum wave function. The basis set is listed for the σ and π continua separately and the center for the orbital [Na denotes the sodium atom (both) and c.m. the center of mass]. See the text for details.

Channel	Center	l	m	Exponent
σ	Na	0	0	64,32,16,8,4,2,1,0.5,0.25,0.125
	Na	1	0	16,8,4,2,1,0.5,0.25,0.125
	c.m.	1	0	4,1,0.25,0.125,0.05
	c.m.	3	0	4,1,0.25,0.125,0.05
	c.m.	5	0	1,0.5,0.25,0.125,0.05
π	Na	1	1	64,32,16,8,4,2,1,0.5,0.25,0.125
	Na	2	1	16,8,4,2,1,0.5,0.25,0.125
	c.m.	1	1	4,1,0.25,0.125,0.05
	c.m.	3	1	4,1,0.25,0.125,0.05
	c.m.	5	1	1,0.5,0.25,0.125,0.05

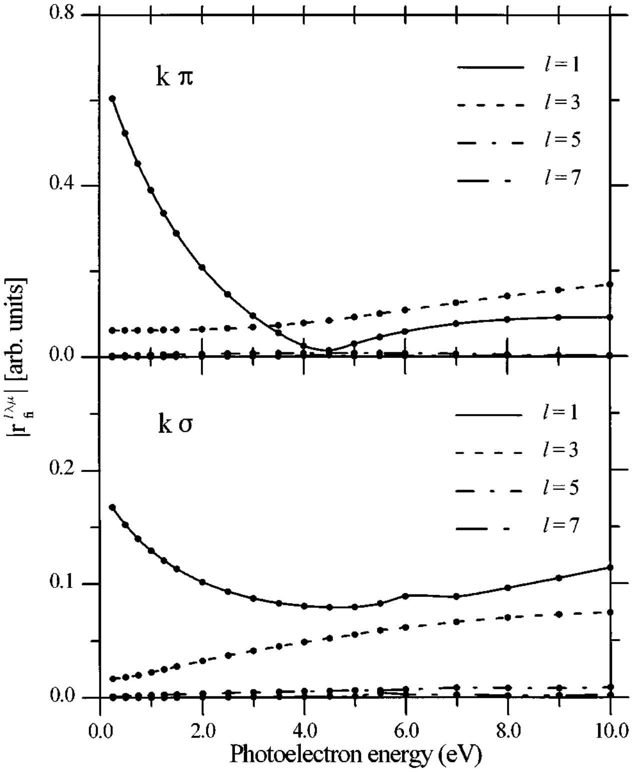

FIG. 1. Absolute value of the dipole matrix element $|r_{ft}^{l\lambda\mu}|$ for $R=6.0$ a.u. as a function of the photoelectron kinetic energy for the various partial waves ($l=1$, 3, 5, and 7) of the $k\sigma$ and $k\pi$ continuum channels, respectively, with the calculated points indicated with a ●. Notice the Cooper minimum in the $k\pi$ channel's $l=1$ wave.

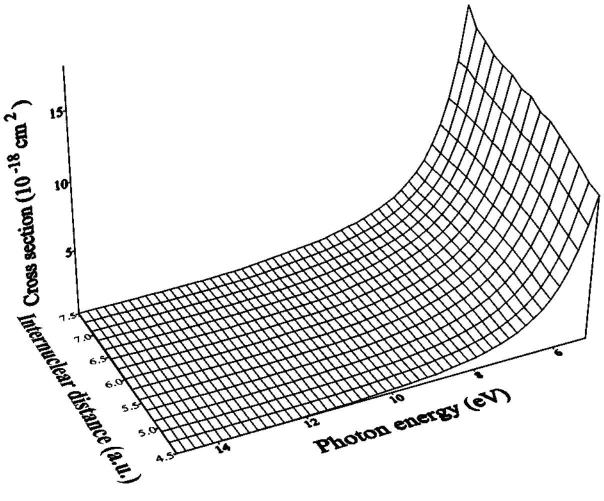

FIG. 2. Calculated photoionization cross section (in 10^{-18} cm^2) as a function of the internuclear distance (in a.u.) and the photon energy (in eV).

averaged cross sections of Eq. (6), $I_{lm\mu}(R,k)$ has been interpolated in k and R using a spline interpolation and the appearance potentials determined using the experimental data of [7] and [10].

The most significant information contained in Fig. 1 is the fact that the p wave of both continuum channels is dominating the photoionization dynamics, as would be predicted from an atomic photoionization picture where the partial wave of the continuum (l) is predicted to differ by ±1 from the bound-state orbital (l_0), i.e., $l=l_0\pm1$ [16]. Since the $4\sigma_g$ state has a predominant $l_0=0$ (s-wave) character, this would predict a dominance of the p wave, as is indeed found. Another important feature seen in Fig. 1 is the Cooper minimum in the $k\pi$-channel's $l=1$ wave around 4.5 eV of photoelectron energy. Although Cooper minima have been experimentally identified for ground-state ionization [17] and recently from excited states [18] and have been predicted in various systems [19–21], it does not, for the present system, lead to a significant influence of the overall photoionization dynamics. This is a result of the molecular nature of the photoionization process, since the effect of the Cooper minimum is ''washed out'' by the presence of the other continuum channels [21]. In Fig. 2 the calculated cross section is shown as a function of the internuclear distance and photon energy. It is seen that the cross section is not strongly dependent on the internuclear distance despite the Cooper minimum, reflecting the strong atomiclike photoionization dynamics and the fact that the $4\sigma_g$ orbital does not have a strong orbital evolution [22] and that the ionic molecular potential does not change dramatically either. The cross section is, however, as expected, seen to be strongly energy dependent, which leads to a rather strong propensity for a Δv that leads to a small photoelectron energy, where Δv is defined as v^+-v.

For the vibrational averaging the one-dimensional Schrödinger equation has been solved, as explained earlier, using the experimentally determined RKR potentials [7,10]. This leads to the Franck-Condon factors listed in Table IV. It is here seen that there is no strong ''simple'' vibrational propensity for most of the vibrational levels, due to the very different potential wells of the neutral and ionic ground states [7,10]. In Fig. 3 the vibrationally resolved photoionization cross sections are shown from the $v=0$, 1, and 2 levels of the ground state, respectively, to various values of v^+. It is seen that the absolute value of the cross section scales, as expected, approximately with the overall Franck-Condon factor for a given v,v^+ combination and that the vibrational branching ratios are not found to vary significantly as a function of the photon energy, except in the near-threshold region where certain ionic vibrational channels close.

In Fig. 4 the calculated photodissociation cross section is shown as a function of the photodissociation laser wavelength for a given ionic vibrational level v^+. The nuclear continuum wave function has been determined using a Nu-

TABLE IV. Calculated Franck-Condon factors between the $X\,^1\Sigma_g^+$ state of Na$_2$(v) and the $X\,^2\Sigma_g^+$ state of Na$_2{}^+$(v^+); see the text for details. Only quantities larger than 5×10^{-5} are listed.

$v\backslash v^+$	0	1	2	3	4	5
0	0.0016	0.0087	0.0253	0.0510	0.0807	0.1070
1	0.0122	0.0476	0.0931	0.1190	0.1070	0.0680
2	0.0445	0.1120	0.1250	0.0706	0.0125	0.0028
3	0.1020	0.1410	0.0577	0.0003	0.0306	0.0672
4	0.1650	0.0913	0.0001	0.0499	0.0703	0.0203
5	0.2000	0.0158	0.0474	0.0748	0.0077	0.0181

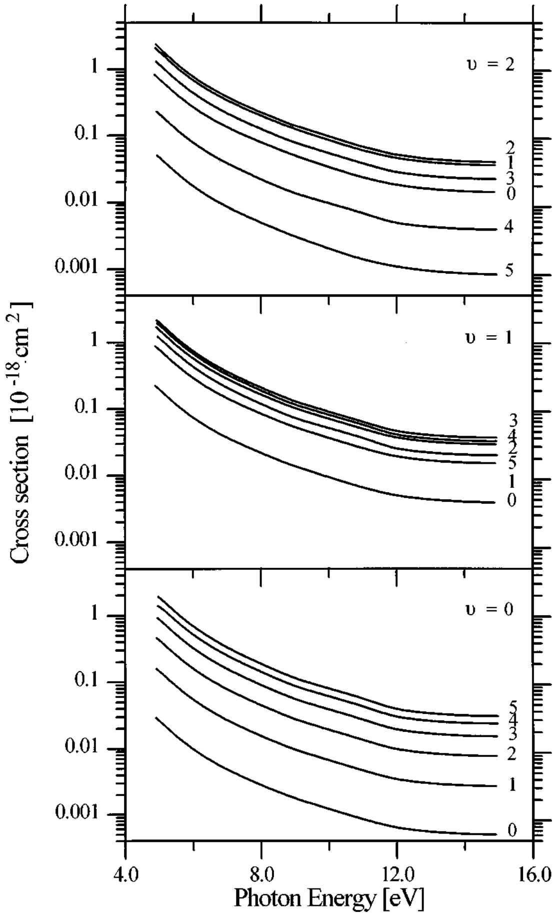

FIG. 3. Vibrationally resolved photoionization cross section (in 10^{-18} cm^2) from the v=0, 1, and 2 levels of the Na$_2$ ground state, respectively, to various values of v^+ as a function of photon energy (in eV).

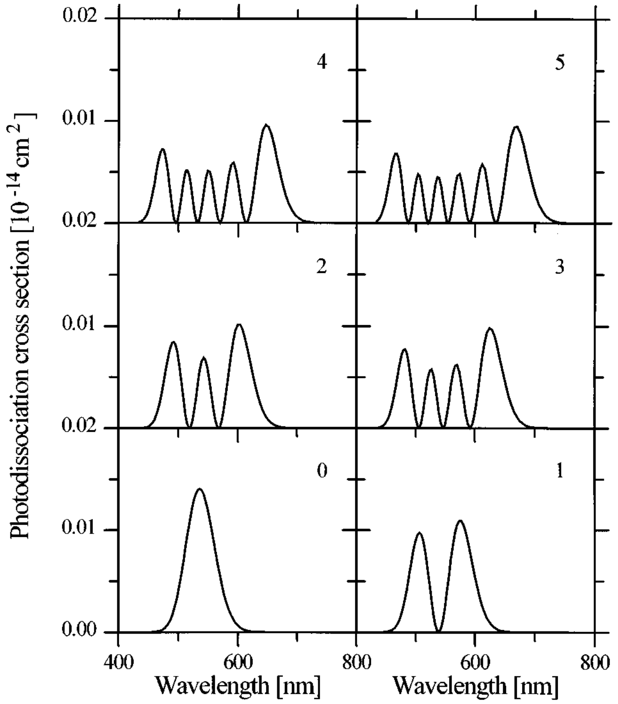

FIG. 4. Calculated photodissociation cross section (in 10^{-14} cm^2) as a function of the photodissociation laser wavelength (in nm) for various ionic vibrational levels.

merov method [15] and the $X\ ^2\Sigma_g^+ \rightarrow 1\ ^2\Sigma_u^+$ dipole matrix element and the potential-energy curves have been taken from Magnier, Dulieu, and Masnou-Seeuws [23] for the determination of the overall photodissociation cross section. Although not strongly varying as a function of internuclear distance, the dipole matrix element does change almost linearly from 2.035 a.u. at R=4.0 a.u. to 2.472 a.u at R=7.0 a.u. [23]. The calculated photodissociation cross sections compare well with the previously calculated values of Dalgarno and co-workers [24], who, for reasons unknown, do not give the cross sections for the v^+=3 level. The absolute value of the cross section, with a maximum value of 1.4×10^{-16} cm^2 at 540 nm for the v^+=0 level, compares well with the experimentally determined value of $(9\pm1)\times10^{-17}$ cm^2 at ~540 nm, recently found by Kortyna *et al.* [7]. This rather large value of the photodissociation cross section is the key issue that made the recent continuous-wave (c.w.) laser experiments feasible that allowed the explicit determination of the ionic vibrational distributions resulting from the thermal associative ionization process [Na($3p$)+Na($3p$)$\rightarrow$Na$_2{}^+$(v^+,J^+)+e^-] [6].

Using the calculated ionic photodissociation cross sections, as depicted in Fig. 4, it is possible to make a least-squares fit to the experimental photodissociation data of Kortyna *et al.* [7] and thereby extract the ionic vibrational distribution. In Fig. 5 the experimental photodissociation data from Kortyna *et al.* [7] and the best least-squares fit (with the ionic vibrational populations as fit parameters and up to v^+=4 included) are shown. This fit leads to a relative ionic vibrational population of 0.633 (v^+=0), 0.015 (v^+=1), 0.243 (v^+=2), 0.103 (v^+=3), and 0.006 (v^+=4), respectively. The quoted experimental errors have been disregarded in the fitting procedure, since the two sets of data from Kortyna *et al.* [7] appear to be statistically inconsistent. The fitted spectrum does not have a very good overall agreement with the measured spectrum, partly due to the fact that some features in the experimental dissociation spectrum (around 550–560 nm) are too "sharp" to be attributed to photodis-

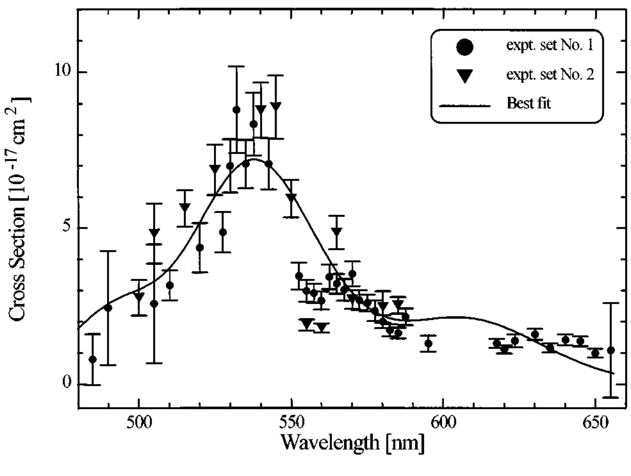

FIG. 5. Experimental photodissociation data from Kortyna *et al.* [7] and the best least-squares fit to these using the calculated photodissociation cross sections with the ionic vibrational populations as fit parameters.

TABLE V. Calculated photoionization cross sections (in 10^{-18} cm^2) for a photon energy equal to the 0-0 adiabatic photoionization threshold energy 4.895 eV. Only cross sections larger than 5×10^{-23} cm^2 are listed.

$v \backslash v^+$	0	1	2	3	4	5
0	0.0293	0	0	0	0	0
1	0.2220	0.8762	0	0	0	0
2	0.7978	2.0334	2.2994	0	0	0
3	1.8066	2.5325	1.0494	0.0055	0	0
4	2.8864	1.6113	0.0014	0.8963	1.2817	0.3764
5	3.4508	0.2751	0.8310	0.9517	0.1410	0.2102

sociation of the molecular ions. These features are present in the experimental spectra despite the great care taken by Kortyna *et al.* [7] to eliminate other sources of Na$^+$ ions. The obvious dominance of the $v^+=0$ level in the ionic distribution from the molecular photoionization is somewhat surprising based on the Franck-Condon factors in Table IV. Despite the fact that the photoionization is done at the wavelength of 253.3 nm ($h\nu=4.895$ eV), corresponding to the 0-0 adiabatic ionization potential of Na$_2$, one would expect a higher ionic vibrational excitation due to the large cross sections for higher vibrational levels, e.g., the $v=1$ to $v^+=1$ cross section, which would dominate at vibrational temperatures higher than 100 K.

In Table V the calculated photoionization cross sections, where both the photoionization dynamics and the vibrational wave functions have been used, are listed as a function of vibrational excitation for a fixed photon energy of 4.895 eV. It is seen that beyond $v=3$ it is energetically possible to have $\Delta v>0$ transitions due to the difference in the vibrational energy of the two states involved (159.8 and 120.7 cm^{-1}, respectively [10,12]). Since the Na$_2$ molecular beam is assumed to have a thermal vibrational distribution with a vibrational temperature of approximately 200 K [7], only about 1% of the population is in $v=4$ or higher. This means that the spectrum is expected to be dominated by transitions with $\Delta v\leqslant0$. Table V also shows that especially photoionization of the $v=2$ level of the ground state of Na$_2$ has a large cross section and that these calculated vibrational branching ratios are somewhat different from the corresponding Franck-Condon factors found in Table IV. By using the vibrational temperature as a fit parameter and the above extracted experimental vibrational distribution combined with the branching ratios of Table V one finds that the molecular beam is much colder (<100 K) than originally estimated by Kortyna *et al.* [7]; see later. Another possible mechanism for the large $v^+=0$ population, besides an initially colder molecular beam, is molecular autoionization through excitation to an electronically doubly excited molecular state [1]. This channel, which is inherently beyond the independent particle description, is not included in the present theoretical description and this may lead to the observed discrepancy, although based on experience from other molecular systems it is not expected to lead to such a dramatic difference [25,26].

To illustrate the sensitivity of the ionic vibrational branching ratios on the initial vibrational temperature we show in Table VI the calculated vibrational ionic branching ratios as a function of temperature for a photon energy of 4.895 eV. The vibrational distribution in the Na$_2$ ground state is assumed to be thermal. It is found that the ionic vibrational branching ratios are rather sensitive to the initial temperature due to the complex vibrational dependence of the ionic branching ratios; see Table V. For vibrational temperatures of less than approximately 70 K the dominant ionic vibrational level is $v^+=0$ and for vibrational temperatures less than approximately 50 K $v^+=0$ is by far the most dominant channel in accordance with the experimental results. A recent reanalysis by Hüwel [27] has shown that their original estimate possibly was too high and that the vibrational temperature certainly was less than 200 K.

In Table VII the calculated ionic branching ratios are shown as a function of the photon energy for a thermal ensemble of Na$_2$ with an assumed vibrational temperature of 200 K following the original estimates of Kortyna *et al.* [7]. It is seen that the ionic vibrational distribution changes radi-

TABLE VI. Calculated ionic vibrational branching ratios as a function of temperature T, assuming a thermal vibrational distribution in the ground state, for a photon energy equal to the 0-0 adiabatic photoionization threshold energy 4.895 eV.

T (K) $\backslash v^+$	0	1	2	3	4	5
50	1.0000	0.2907	0.0077	0.0000	0.0000	0.0000
100	0.5531	1.0000	0.2196	0.0010	0.0012	0.0004
150	0.4486	1.0000	0.3787	0.0080	0.0092	0.0030
200	0.4792	1.0000	0.4615	0.0214	0.0233	0.0078
250	0.5336	1.0000	0.5030	0.0375	0.0389	0.0134
300	0.5898	1.0000	0.5251	0.0537	0.0535	0.0188
350	0.6419	1.0000	0.5376	0.0687	0.0664	0.0238
400	0.6885	1.0000	0.5452	0.0823	0.0777	0.0282
450	0.7297	1.0000	0.5501	0.0944	0.0873	0.0321

TABLE VII. Calculated ionic vibrational branching ratios as a function of photoionization photon energy (in eV) for ionization of a thermal distribution of Na_2 molecules with a vibrational temperature of 200 K. Note that the first two energies are below the 0-0 adiabatic photoionization threshold energy of 4.895 eV and thus are dominated by photoionization from higher vibrational states of the ground state. Only up to $v=5$ has been included in the calculation.

$h\nu$ (eV) \ v^+	0	1	2	3	4	5
4.800	1.0000	0.0000	0.0000	0.0000	0.0000	0.0000
4.850	1.0000	0.1757	0.0275	0.0299	0.0000	0.0000
4.895	0.4792	1.0000	0.4615	0.0214	0.0233	0.0078
5.000	0.1523	0.4076	0.6901	1.0000	0.0074	0.0025
5.250	0.1085	0.2904	0.5054	0.7150	0.8877	1.0000
5.500	0.1093	0.2922	0.5077	0.7176	0.8867	1.0000
5.750	0.0984	0.2934	0.5091	0.7185	0.8880	1.0000
6.000	0.1108	0.2955	0.5119	0.7212	0.8839	1.0000
6.500	0.1133	0.2354	0.5181	0.7263	0.8924	1.0000

cally as function of energy and that at photon energies larger than 5 eV it leads to a significant population inversion as found for the associative ionization process [6]. With this in mind, it is clear that one is not able solely on basis of the ionic vibrational branching ratios to determine whether the direct photoionization mechanism or a molecular autoionization mechanism is the primary channel for associative ionization at ultraslow collision velocities (photoassociated ionization) [28–30]. For photon energies under the 0-0 threshold a larger relative $v^+=0$ population is found, simply because this is solely dominated by photoionization from thermally populated higher vibrational states of the ground state. Although it is inconceivable that this would be the case in the experiments of Kortyna *et al.* [7], the use of a photon energy 0.05 eV less than the 0-0 threshold would lead to a similar ionic vibrational distribution as found for a colder molecular beam ($T_{\mathrm{vib}} \approx 50$ K).

In Fig. 6 the calculated photodissociation spectrum of ions resulting from photoionization at a photon energy of 4.895 eV of an assumed thermal ($T_{\mathrm{vib}}=50$ and 200 K) Na_2 beam is shown. Here the calculated vibrationally resolved photoionization cross sections and the calculated photodissociation cross sections have both been combined in the total calculation. The experimental points of Kortyna *et al.* [7] are also shown in Fig. 6. It is seen that the agreement between the theoretical and the experimental values is rather poor for an assumed vibrational temperature of 200 K, since at this temperature there is a substantial vibrational excitation in the neutral atoms as explained above. However, if one assumes that the vibrational temperature is much lower than originally estimated, the agreement between the calculated and measured spectra increases dramatically, as can be seen in Fig. 6 for a vibrational temperature of 50 K. This is in general agreement with the recent reanalysis by Kortyna *et al.* [27] of the initial vibrational temperature in their experiment [7].

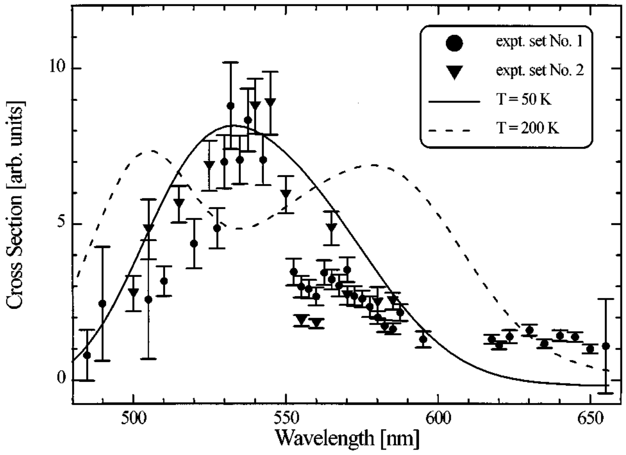

FIG. 6. Calculated photodissociation spectrum of ions resulting from photoionization of Na_2 with 4.8948-eV photons, corresponding to the adiabatic photoionization potential of Na_2, with a vibrational temperature of $T_{\mathrm{vib}}=50$ and 200 K.

IV. CONCLUSION

We have presented a purely *ab initio* calculation of the photoionization process from the ground state of Na_2 followed by photodissociation of the resulting ions. For the photoionization a Cooper minimum was found in the $k\pi$-continuum's p wave ($l=1$) around a photoelectron energy of approximately 4.5 eV. This is not found to lead to significant observable implications for the total cross sections. The total photoionization cross section is found to be strongly energy dependent and decreasing rapidly for increasing photoelectron energy. The calculated cross sections are, however, not found to be strongly dependent of the internuclear distance and there is not a significant orbital evolution of the ground-state valence orbitals as a function of internuclear distance.

Despite the relatively weak internuclear dependence of the photoionization cross section, the ionic vibrational branching ratios are found to depart significantly from the corresponding Franck-Condon factors. This is primarily due to the strong energy dependence of the cross sections, since the final photoelectron kinetic energy, for a given photon frequency, will be different for the various vibrational levels. The ionic branching ratios are found to be strongly dependent on the photon frequency around and just under the 0-0 ionization threshold, but to a lesser degree at larger photon energies.

The calculated wavelength-dependent photodissociation cross sections are found to be in good agreement with previously published theoretical results where a comparison was possible. The recently determined absolute cross sections are also, according to the present calculation, within the experimental error [7]. The combination of the calculated photoionization cross sections and the photodissociation cross sections makes it possible, under the assumption of a given thermal distribution in the ground state of Na_2, to predict the resulting normalized ion yield as a function of the photodissociation laser wavelength. A change in the assumed thermal distribution leads to a dramatic change in the spectrum due to the complex change in the ionic vibrational distributions as a function of photoionization energy and vibrational excitation. A vibrational temperature of 50 K leads to relatively good agreement with the experimental results [7].

Some of the very sharp features found in the experimental results are not found in the calculated photodissociation spectra and these are not presumed to stem from the photodissociation of Na_2^+ ions. As seen in Fig. 4, these features are simply too sharp to correspond to photodissociation of a lower-lying vibrational level. If higher vibrational states were responsible for this structure, then other easily recognizable features would have to be present in the photodissociation spectrum at other wavelengths. Despite the care taken by Kortyna *et al.* [7], they were unable to exclude this source of Na^+ ions and we are presently unable to assign it to any diatomic process.

The possible influence of molecular autoionization on the ionic vibrational branching ratios, which has not been included in the present theoretical description, is intriguing, especially since this is directly comparable to the experiments [1,3,6,28–30] with laser-cooled Na atoms, where it is not yet obvious whether photoionization or molecular autoionization is the dominant mechanism for the creation of the Na_2^+ ions. Doing a wavelength-dependent photoionization experiment would therefore be important, since molecular autoionization features are expected to be rather sharp. The vibrational branching ratios should therefore be even more dependent on the photon energy than found in the present work. The experimental choice for the photon energy for the ionization step [7] turns out to be rather unfortunate, since the cross sections are so strongly varying around the threshold due to the small vibrational constants of the states involved and due to the complex vibrational overlap between the ion ground state and the neutral ground state.

The present work suggests that there are other combinations of vibrational temperature and photoionization photon energy that will also lead to a peaked ionic vibrational distribution, i.e., where one vibrational ion state is predominantly populated, and this may be used for further experiments where a specific ionic vibrational state is desired. For future experiments and comparison with theory it is, however, very important to have a good determination of the ground-state vibrational temperature (distribution), since it has significant implications on the final ionic vibrational distributions. It is possible that this can be achieved via photoassociation of laser-cooled atoms [30], combined with optical pumping to a given vibrational level of the ground state of Na_2. An alternative would be to use a multiphoton scheme going through excited states of the Na_2 molecule and by that achieving the desired vibrational (and rotational) selectivity.

ACKNOWLEDGMENTS

The authors are happy to acknowledge the helpful discussions with Olivier Dulieu, Lutz Hüwel, Diane Lynch, Françoise Masnou-Seeuws, and Vince McKoy. The authors would also like to acknowledge the help of S. Magnier by providing her results on Na_2^+ prior to publication and J. J. Blangé with the fit to the experimental data. This work has been supported by the ‘‘Stichting voor Fundamenteel Onderzoek der Materie,’’ which is financially supported by the ‘‘Nederlandse Organisatie voor Wetenschappelijk Onderzoek.’’ This work has furthermore been partially supported by the European Union’s Human Capital and Mobility Programme under Contract No. ERBCHRXCT930344.

[1] J. Weiner, F. Masnou-Seeuws, and A. Giusti-Suzor, Adv. At. Mol. Phys. **26**, 209 (1989).
[2] H. A. J. Meijer, T. J. C. Pelgrim, H. G. M. Heideman, R. Morgenstern, and N. O. Andersen, J. Chem. Phys. **90**, 738 (1989).
[3] H. A. J. Meijer, S. Schohl, M. W. Muller, H. Dengel, M.-W. Ruf, and H. Hotop, J. Phys. B **24**, 3621 (1991).
[4] J. H. Nijland, J. A. de Gouw, H. A. Dijkerman, and H. G. M. Heideman, J. Phys. B **25**, 2841 (1992).
[5] J. H. Nijland, J. J. Blangé, H. Rudolph, H. A. Dijkerman, and H. G. M. Heideman, J. Phys. B **25**, 4835 (1992).
[6] X. Urbain, J. J. Blangé, H. A. Dijkerman, H. Rudolph, and H. G. M. Heideman, J. Phys. B **27**, L245 (1994).
[7] A. Kortyna, D. Reisner, J. Unruh, and L. Hüwel, Phys. Rev. A **50**, 1399 (1994).
[8] R. R. Lucchese, R. Raseev, and V. McKoy, Phys. Rev. A **25**, 2572 (1982).
[9] R. R. Lucchese, K. Takatsuka, and V. McKoy, Phys. Rep. **131**, 147 (1986).
[10] P. Kuch and M. M. Hessel, J. Chem. Phys. **68**, 2591 (1978).
[11] M. W. Schmidt, K. K. Baldridge, J. A. Boatz, J. H. Jensen, S. Koseki, M. S. Gordon, K. A. Nguyen, T. L. Windus, and S. T. Elbert, QCPE Bull. **10**, 52 (1990).
[12] R. F. Barrow, J. Verges, C. Effantin, K. Hussein, and J. d’Incan, Chem. Phys. Lett. **104**, 179 (1984).
[13] D. L. Lynch, S. N. Dixit, and V. McKoy, J. Chem. Phys. **84**, 5504 (1986).
[14] M. Braunstein and V. McKoy, J. Chem. Phys. **87**, 224 (1987).
[15] B. R. Johnson, J. Chem. Phys. **67**, 4086 (1977).
[16] H. Rudolph, S. N. Dixit, V. McKoy, and W. M. Huo, J. Phys. Chem. **88**, 637 (1988).
[17] T. A. Carlson, M. O. Krause, W. A. Svenson, P. Gerard, F. A. Grimm, T. A. Witley, and B. P. Pullen, Z. Phys. D **2**, 309 (1986).
[18] H. Park and R. N. Zare, Chem. Phys. Lett. **225**, 327 (1994).
[19] J. A. Stephens and V. McKoy, Phys. Rev. Lett. **62**, 889 (1989).
[20] J. A. Stephens, M. Braunstein, V. McKoy, H. Rudolph, and M.-T. Lee, Phys. Scr. **41**, 482 (1990).

[21] H. Rudolph, R. L. Dubs, and V. McKoy, J. Chem. Phys. **93**, 7513 (1990).

[22] H. Rudolph and V. McKoy, J. Chem. Phys. **91**, 1374 (1989).

[23] S. Magnier, O. Dulieu, and F. Masnou-Seeuws (private communication).

[24] T. Uzer and A. Dalgarno, Chem. Phys. Lett. **61**, 213 (1979); K. Kirby-Docken, C. J. Cerjan, and A. Dalgarno, *ibid*. **40**, 205 (1976).

[25] H. Rudolph, D. L. Lynch, S. N. Dixit, V. McKoy, and W. M. Huo, J. Chem. Phys. **86**, 1748 (1987).

[26] C. Cornaggia, A. Giusti-Suzor, and Ch. Jungen, J. Chem. Phys. **87**, 3934 (1987).

[27] L. Hüwel (private communication). The vibrational temperature of the Na_2 ground state is estimated to be 125±25 K.

[28] R. Napolitano, J. Weiner, C. J. Williams, and P. S. Julienne, Phys. Rev. Lett. **73**, 1352 (1994).

[29] R. A. Cline, J. D. Miller, and D. J. Heinzen, Phys. Rev. Lett. **73**, 632 (1994).

[30] L. P. Ratliff, M. E. Wagshul, P. D. Lett, S. L. Rolston, and W. D. Phillips, J. Chem. Phys. **101**, 2638 (1994).